Domain wall motion in nanopillar spin-valves with perpendicular anisotropy driven by spin-transfer torques

J. Cucchiara,[1] S. Le Gall,[1] E. E. Fullerton,[2] J.-V. Kim,[3] D. Ravelosona,[3] Y. Henry,[4] J. A. Katine,[5] A. D. Kent,[6] D. Bedau,[6] D. Gopman,[6] and S. Mangin[1]

[1]*Institut Jean Lamour, Université de Lorraine UMR CNRS 7198, Vandoeuvre lès Nancy, France*
[2]*Center for Magnetic Recording Research, University of California San Diego, La Jolla, California 92093-0401, USA*
[3]*Institut d'Electronique Fondamentale, UMR CNRS 8622, Université Paris Sud, France*
[4]*Institut de Physique et Chimie des Matériaux de Strasbourg, CNRS, UDS, Strasbourg, France*
[5]*HGST San Jose Research Center, San Jose, California, USA*
[6]*Department of Physics, New York University, New York, New York 10003, USA*

(Received 18 June 2012; revised manuscript received 28 September 2012; published 28 December 2012)

Using transport measurements and micromagnetic simulations we have investigated the domain wall motion driven by spin-transfer torques in all-perpendicular hexagonal nanopillar spin-valves. In particular, we probe domain walls nucleated in the free layer of the spin-valves, which are then pinned in the devices. We have determined both the field-current state diagrams for the domain-wall state and the thermally activated dynamics of the nucleation and depinning processes. We show that the nucleation process is well-described by a modified Néel-Brown model taking into account the spin-transfer torque, whereas the depinning process is independent of the current. This is confirmed by an analytical calculation which shows that spin-torques have no effect on the Arrhenius escape rate associated with thermally activated domain wall depinning in this geometry. Furthermore, micromagnetic simulations indicate that spin-transfer only weakly affects the domain wall motion, but instead modifies the inner domain wall structure.

DOI: 10.1103/PhysRevB.86.214429 PACS number(s): 85.75.Bb, 75.47.De, 75.60.Ch, 75.60.Lr

The first works related to spin-transfer were carried out in the late 1970s when Berger predicted that spin-current should be able to move a magnetic domain wall.[1] But only in the late 1990s, thanks to huge progress in nanofabrication techniques, current induced reversal were theoretically[2] and experimentally[3–6] studied. This spin-transfer torque phenomena are now well documented in review papers as Ref. 7.

Nowadays, the controlled nucleation, propagation, pinning, and depinning of domain walls (DWs) by a spin-polarized current has become an extensive field of study.[8,9] These phenomena involve fundamental questions concerning the interplay between spin transport and magnetization dynamics, and have led to proposals for possible applications in magnetic logic[10] and multistate memories.[11] Most of the studies to date have been focused on current-in-plane (CIP) spin torques, in which the applied current flows along the propagation direction of the DW.[12–14] In this scenario the interaction of the spin of the conduction electrons with the spatially inhomogeneous magnetization leads to a torque on the domain wall. The resulting DW dynamics are largely determined by the relative weight of the adiabatic and nonadiabatic processes, where in the latter the spin-transfer torques play the role of an applied field.[43]

Recent studies have shown that domain wall dynamics can also be strongly influenced by spin torques from currents perpendicular to the plane (CPP) in spin-valves or magnetic tunnel junctions.[15–18] These torques arise from the transfer of spin angular momentum between the free and reference magnetic layers, where the details of the torque depends very much on the material composition and transport properties of the multilayer structure. It has been shown that a judicious choice of the reference layer magnetization configuration can lead to drastic changes to the critical currents for DW motion and the DW velocities.[11–15] In nanopillar spin-valves with perpendicular magnetic anisotropy, DWs within the free layer of the structure can be manipulated for a large range of magnetic fields and currents.[18–21] These devices are therefore of great interest for studying the impact of spin-polarized currents on DW dynamics in the CPP geometry, which is not possible in standard nanowire geometries.[22,23]

In this article we investigate the room-temperature dynamics of a single DW located in the free layer of a nanopillar spin-valve with perpendicular anisotropy, for fields and dc currents applied perpendicular to the film plane. This study focuses on the micromagnetic state formed by a single DW pinned on a defect in the devices, leading to a spin-valve configuration halfway between the parallel (P) and the antiparallel (AP) states. We report on the nucleation and depinning processes associated with this intermediate DW state under a wide range of magnetic fields and currents by measuring field-current state diagrams. We further consider the influence of fields and currents on the thermally activated nucleation and propagation events by analyzing random telegraph noise signals recorded at room temperature between this DW state and the uniformly magnetized P or AP states.

The nanopillars used for this study were grown by evaporation and dc magnetron sputtering as described in Ref. 24. Their magnetic structure consists of a Pt (3 nm)/[Co (0.25 nm)/Pt (0.52 nm)] × 5/Co (0.2 nm)/[Ni (0.6 nm)/Co (0.1 nm)] × 2/Co (0.1 nm) reference layer and a Co (0.1 nm)/[Co (0.1 nm)/Ni (0.6 nm)] × 4 free layer separated by a 4 nm spacer of copper. These multilayered films were then patterned into nanopillars forming elongated 200 × 100 nm^2 hexagons. The magnetic behavior is monitored through dc and ac resistance measurements. The current is defined as positive when the electrons flow from the reference layer to the free layer supporting the P state. The reference layer switches for an

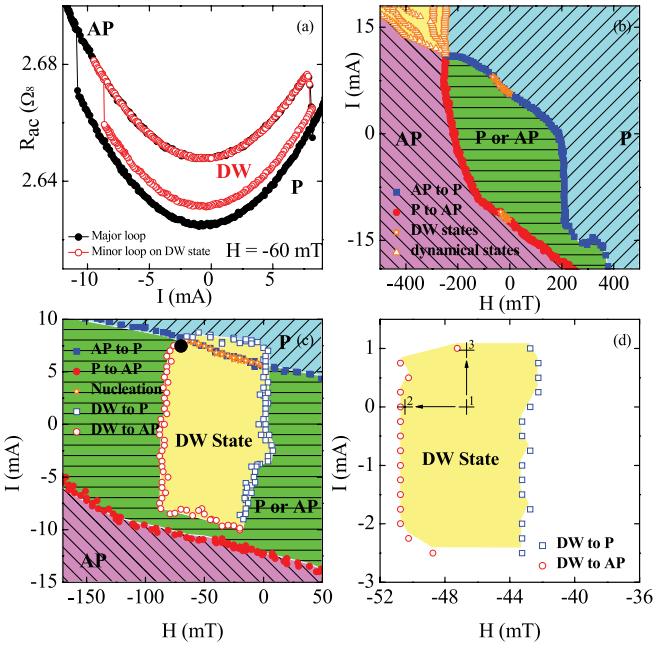

FIG. 1. (Color online) (a) Resistance of a 200 × 100 nm^2 hexagonal nanopillar spin-valve as a function of the injected current. The solids circles are for a major hysteresis loop. The opened red circles are for a minor hysteresis loop between the P state and a DW state formed by a single DW pinned in the free layer. (b) Experimental state diagram (magnetic field H vs injected current I) obtained from major hysteresis loops such as the one of (a). Four regions are visible: One for the P state, one for the AP state, a bistability region, and a region where dynamical state are expected. (c) On top of the previous state diagram, the experimental state diagram of the DW state formed by a single DW pinned in the free layer obtained from minor hysteresis loops (a). The black circle indicates the region corresponding to the measurements of the telegraph noise signals on a similar sample and presented in Fig. 2. (d) Calculated state diagram of a DW state formed by a single pinned DW in the free layer (micromagnetic simulation).

applied magnetic field of about 1 T, so it can be considered as fixed for all the experiments presented here. The applied magnetic field H is then defined as positive when it is applied in the same direction as the reference layer magnetization.

The state diagram we consider represents the available magnetic states of the spin-valve as a function of the H and the injected current.[24–26] It is constructed from field hysteresis loops measured at different injected currents or current hysteresis loops measured at different H. Figure 1(a) presents two current hysteresis loops measured for one device at $H = -60$ mT. Solid circles indicate the major hysteresis loop showing transitions between the P and the AP states. Red open circles depict a minor hysteresis loop between the AP state and a DW state consisting of a single DW pinned in the device. The presence of such DW state was demonstrated using angle dependent measurements[18] and imaging.[21] Figure 1(b) shows the state diagram of this device obtained from major hysteresis loops such as the one presented in Fig. 1(a). The solid blue squares (red circles) mark the transition between the uniformly magnetized states from AP to P (P to AP). In Fig. 1(b) we identify four distinct regions representing different micromagnetic states of the spin valve, as predicted and shown previously:[24–27] Stable AP state on the right, stable P state on the left, bistable P or AP states in the center, and a free layer dynamical state in the upper left corner. The presence of such dynamical states has been predicted[24,25,27] and also experimentally evidenced recently.[28,29] Figure 1(c) shows the state diagram of the DW state, consisting of a single DW pinned in the device, obtained from minor hysteresis loops such as the one presented in Fig. 1(a). Starting from the AP state, a DW can be nucleated once the system reaches the border denoted by orange open stars. These symbols mean that the DW has indeed been nucleated and pinned in the free layer, leading to an intermediate resistance level between the resistance of the P and of the AP states in the corresponding hysteresis loops.[18–20] As soon as this DW state is created the magnetic field and the injected current can be swept to determine the DW state stability region. The blue open squares (red circles) mark a transition from the DW state to the P (AP) state. The yellow area delimited by these borders corresponds to the existence region of the DW state.

To gain a fuller understanding of these results, and to ensure that they are not specific to the particular device studied but rather characteristic of this DW state, we performed micromagnetic simulations of our system including the Slonczewski spin-torque term.[30] We assumed a 200 × 100 nm^2 hexagonal element where the reference layer was 6 nm thick and the free layer 3 nm thick separated by 3 nm nonmagnetic spacer layer. The elementary cells were 4 × 4 × 3 nm^3 rectangular cuboid. The reference layer had a saturation magnetization $M_s = 5 \times 10^5$ A m^{-1} and a perpendicular uniaxial anisotropy constant $K_u = 3.3 \times 10^5$ J m^{-3}. The free layer parameters were $M_s = 6.5 \times 10^5$ A m^{-1} and $K_u = 2.5 \times 10^5$ J m^{-3}. For both layers the intralayer exchange between cells was 2×10^{-11} J m^{-1}, the polarization 0.35 and the damping coefficient 0.1. The calculations were performed assuming zero temperature. Inside the free layer, close to its center at the coordinates $(x,y) = (94$ nm, 54 nm), we defined an artificial defect by a 16 × 16 × 3 nm^3 rectangular cuboid with $K_u = 1.25 \times 10^5$ J m^{-3}, that is, the anisotropy is reduced by a factor of 2 compared to the other cells of the layer.

The micromagnetic domain wall configuration was obtained by relaxing the system from an initial state of two opposite domains oriented perpendicular to the film plane with a sharp domain wall in the center. To compensate for the dipolar field from the reference layer, a magnetic field of $Hz = -47$ mT was applied during the simulations. The micromagnetic calculations reveal a Néel wall structure, in agreement with the parameters used for these simulations: The quality factor of the free layer $Q = 2K_u/\mu_0 M_s^2 = 0.94$ is slightly smaller than 1 and therefore a Néel wall is expected to have a lower energy than a Bloch wall. Note that Q is nevertheless close to 1. This micromagnetic state was then used as the initial configuration for the applied field and current sweeps were used to determine the state diagram, in particular, to compute the boundaries for domain wall stability. Figure 1(d) shows the calculated state diagram we obtained. The shape of the existence region shows qualitative agreement with the experimental results.

The slope of the experimental nucleation border [orange stars in Fig. 1(c)] reveals that the nucleation process of a DW in nanopillar spin-valves with perpendicular anisotropy

is affected both by the applied magnetic field and the injected spin-polarized current. We can make a similar argument for the field and current dependence of the depinning process by looking at the boundaries of the existence region of the DW state {measurement [Fig. 1(c)] and the calculation [Fig. 1(d)]}. The upper and lower boundaries follow the slope of the borders marking the transition between the uniformly magnetized states. This indicates that the applied magnetic field affects the depinning process of the DW. However, the left and right boundaries are nearly vertical and parallel to the current axis. This indicates that the spin-polarized current does not modify the depinning field of the DW.

To fully examine the impact of the applied magnetic field and of the injected spin-polarized current, and also to consider the effect of thermal activation on the stability of a DW state formed by a single pinned DW in the free layer, we studied another type of sample for which the free layer has a weaker anisotropy and is therefore less thermally stable. This type of sample (described elsewhere[31]) allows for thermally activated processes at room temperature to be studied[32] by measuring the telegraph noise[33] from transitions between a DW state and the P state. Those signals generally appear at the corner of the existence regions for the DW state, indicated by the solid black circle in Fig. 1(c), where the spin-valve free layer switches back and forth between different magnetic configurations as a result of thermal activation. This phenomenon is reflected in a stochastic switching of the resistance level of the devices as a function of time as shown in the inset of Fig. 2(d). From these signals, the mean lifetime of the magnetic states involved can be extracted, as detailed elsewhere.[33] The analysis of their evolution as a function of the applied magnetic field and spin-polarized current for the P and the DW states allows probing the nucleation and the depinning processes. Indeed, the transition from the P to the DW state involves nucleation, whereas the transition from the DW to the P state involves depinning (and subsequent propagation) of the DW. The process studied may therefore be described as a thermally activated single energy barrier crossing with no memory effect, as shown for other DW depinning processes.[34,35] This telegraph noise behavior is a slow dynamic regime (from several seconds to a few minutes) in which thermal activation plays an important role, in contrast to the faster dynamic regime (below few milliseconds) in which other phenomena dominate.[36–38]

Figures 2(a) and 2(b) present the evolution of the mean dwell time of the P state as a function of the applied magnetic field for different injected spin-polarized currents, and of the injected spin-polarized current for different applied magnetic fields, respectively. Both the magnetic field and the current lead to an exponential variation of the mean dwell time of the P state. The mean dwell time increases with the applied magnetic field and with the injected current, which is in agreement with the fact that a positive field or current favors the P state. As a consequence, both field and current affect the energy that the system receives and the energy barrier that it has to cross in order to nucleate a domain and create a DW. This is in agreement with the slope observed in the experimental nucleation border in Fig. 1(c).

The linear slope (on the logarithmic scale) of the field and current dependence of the mean dwell time of the P state appears to be largely independent of the current

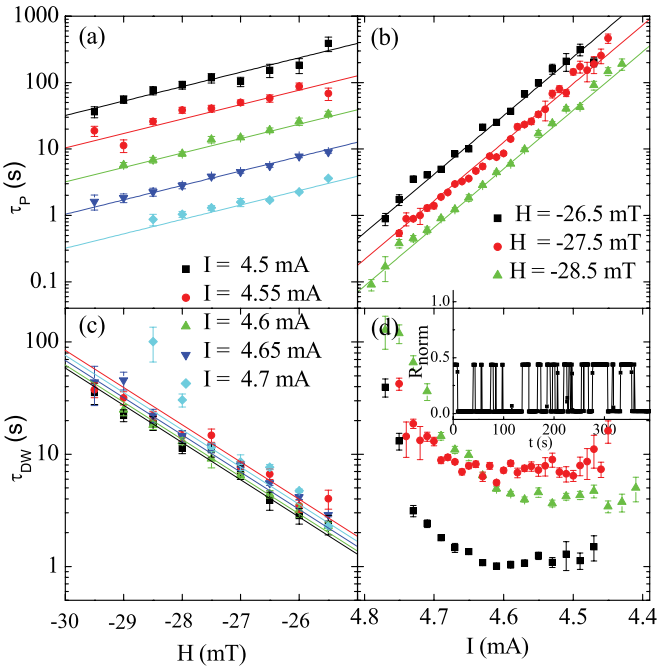

FIG. 2. (Color online) (a) Evolution of the P state mean dwell time as a function of the applied magnetic field for different currents. (b) Evolution of the P state mean dwell time as a function of the current for different applied magnetic fields. (c) Evolution of the DW state mean dwell time as a function of the applied magnetic field for different currents. (d) Evolution of the DW state mean dwell time as a function of the current for different applied magnetic fields. Inset: Telegraph noise signal. Evolution of the normalized resistance of a device as a function of time for $H = -28$ mT and $I = 4.6$ mA. The lines are guides for the eyes.

(field) [Figs. 2(a) and 2(b)]. From this observation, the evolution of the mean dwell time of a uniformly magnetized state can be modeled by a modified Arrhenius law $\tau = \tau_0 \exp[2M_s V_n(H + H_n + \varepsilon I)/k_B T]$, where τ_0 is the attempt time of the system, V_n is its nucleation volume, H_n is its nucleation field, and ε is a spin-transfer efficiency factor that converts the applied current into an effective magnetic field. Taking a reasonable order of magnitude for the attempt time $\tau_0 = 10^{-10}$ s and a saturation magnetization obtained from magnetic measurements $M_s = 6.5 \times 10^5$ A m^{-1}, a fit of these curves gives reasonable values for the other parameters of the equation: $V_n = 1500$ nm^3 (about 4 % of the total volume of the free layer), $H_n = 200$ mT (in agreement with the anisotropy constant $K_u \sim 2M_s V_n = 2.5 \times 10^5$ J m^{-3} obtained from magnetic measurements), and $\varepsilon = 40$ T A^{-1} (in agreement with the slope of the experimental state diagram). Considering a linear evolution of the energy barrier of the system as a function of the applied magnetic field $E_b(H) = 2M_s V_n (H + H_n)$,[39,40] the modified Néel-Brown law presented in the literature[41] may seem quite different from the expression we used for the mean dwell time since this energy barrier should be multiplied by a linear function of the current in the numerator of the exponential. However, given the small field and current ranges in which the telegraph noise signals are observed, a first-order approximation of this modified Néel-Brown law, in agreement with the expression we used, is sufficient.

Figures 2(c) and 2(d) show the mean dwell time of the DW state as a function of field or current. In Fig. 2(c) the mean dwell time exhibits an exponential variation with the applied magnetic field for currents below 4.65 mA (in absolute value). The current has no effect on these curves until it reaches 4.7 mA (normal to the film), after which a sharper increase in the mean dwell time is observed with decreasing magnetic field. This phenomenon is confirmed in Fig. 2(d), where the mean dwell times remain constant with the injected current below 4.65 mA (in absolute value) and increase nonlinearly above this value for the three applied magnetic field values presented here. This large increase seems to contradict the DW state diagram presented previously since larger negative currents are expected to favor the disappearance of the DW state, thereby leading to a decrease in the mean dwell time. However, these curves are extracted from telegraph noise signals measured between the P and the DW state. Under these conditions, the P state is less favorable (and therefore less stable) than the DW state, which leads to the dwell time of the P state decreasing faster than that for the DW state. As such, the increase in the dwell time of the DW state under large negative currents reflects the fact that the P state loses stability faster than the DW state.

The weak dependence of the mean dwell time of the DW state with the injected current suggests that the spin-polarized current leaves the energy landscape defined by the pinning site largely unaffected and has little impact on the depinning process. On the contrary, the magnetic field modifies the energy landscape of the system and so affects the depinning process.

The qualitative features of the current dependence of the dwell time can be understood in terms of a 1D model for domain wall dynamics.[42,43] We consider the following dynamics for the free layer magnetization:

$$\frac{d\mathbf{m}}{dt} = -|\gamma_0|\mathbf{m}\times\mathbf{H}_{\text{eff}} + \alpha\mathbf{m}\times\frac{d\mathbf{m}}{dt} - \sigma I\,\mathbf{m}\times(\mathbf{m}\times\mathbf{p}), \tag{1}$$

where $\mathbf{m}$ is a unit vector representing the local magnetization orientation. The first term on the right-hand side describes precession about the local effective field $\mathbf{H}_{\text{eff}}$, where γ_0 is the gyromagnetic constant. The second term represents Gilbert (viscous) damping that is parametrized by the dimensionless constant α. The third term represents the action of CPP spin torques, where $\mathbf{p}$ is a unit vector representing the orientation of the reference layer magnetization, σ is the spin-transfer efficiency, and I is the applied current. The latter represents the "sine" approximation of the spin torques, which suffices to illustrate the general behavior we observe. We assume a Néel wall profile of the form

$$\theta(x) = 2\tan^{-1}\exp\left[\frac{x - X_0(t)}{\lambda}\right], \tag{2a}$$

$$\phi(x) = \phi_0(t), \tag{2b}$$

where x represents the long axis of the nanopillar and z is the direction perpendicular to the film plane, θ and ϕ represent the magnetization orientation in spherical coordinates, and λ is the Néel wall parameter $\lambda = \sqrt{A/K_{u,\text{eff}}}$, where the effective anisotropy is $K_{u,\text{eff}} = K_u - \frac{1}{2}\mu_0 M_s^2$. For a uniform reference layer magnetization $\mathbf{p} = \mathbf{z}$ we can derive the equations of motion for the dynamical Néel wall variables X_0(t) and ϕ(t) from Eq. (1) after integrating over the free layer volume:

$$-\frac{\dot{X}_0}{\lambda} + \alpha\dot{\phi}_0 = \frac{1}{2}\gamma_0 M_s \sin(2\phi_0) + \sigma I, \tag{3a}$$

$$\dot{\phi}_0 + \frac{\alpha\dot{X}_0}{\lambda} = \gamma_0 H, \tag{3b}$$

where H is the applied magnetic field along the z axis. By comparing Eq. (3) with the equations of motion for a Néel wall under CIP spin torques, we observe that the CPP torque in our geometry has the same action as an adiabatic spin torque in the case of CIP-driven domain wall dynamics, where σI is equivalent to u/λ with u being an effective spin-drift velocity.[43] However, in contrast to wall dynamics in in-plane magnetized free layers,[15,17] no equivalent nonadiabatic CIP torques are introduced by the CPP currents in the present case. If only adiabatic torques are present we do not expect any changes to the rate of thermally activated depinning,[42] which is consistent with our experimental results.

To further clarify the action of spin-transfer torques on the DW state, we examined the evolution the domain wall using micromagnetic simulations after applying a field or current step. For times t < 0 we initialize the spin-valve in the DW state in its equilibrium configuration for $H = -47$ mT and $I = 0$ mA, which is at the center of the DW existence region. At $t = 0$ we apply different fields or currents within the existence region for the DW state but sufficiently close to the region borders such that transitions toward a different equilibrium magnetic configuration can be initiated.

The time evolution of the magnetization after switching the magnetic field showed that in a few nanoseconds the system reaches a new equilibrium corresponding to a slightly shifted but otherwise unchanged Néel wall. We conclude, therefore, that the applied magnetic field initiates the depinning process of the DW.

The time evolution of the magnetization after application of a 1 mA current shows that in about 120 ns the system reaches a new equilibrium state that, in contrast to the previous case, is a DW at the same position, but with its internal structure modified. Indeed, the magnetic moments inside the DW rotate in the plane of the layer and its structure becomes closer to a Bloch wall. Note that the transition from a Néel to a Bloch wall profile is plausible given that the quality factor of the free layer $Q = 0.94$ is close to 1. Therefore, it appears that the spin-transfer torque does not depin or even move the domain wall, but only modifies its internal micromagnetic structure. This is consistent with the observation that the spin-transfer torque has virtually no effect on the field-current state diagram or on the mean dwell time of the DW state.

In summary, we have presented an experimental and theoretical study of the nucleation and depinning processes of a single DW in the free layer of nanopillar spin-valves with perpendicular anisotropy, under the influence of magnetic fields and spin-polarized currents perpendicular to the film plane. We characterized the devices by measuring their state diagrams and the telegraph noise emitted by transitions between a uniform and a domain wall state. The nucleation process of the domain wall is found to be strongly dependent on the applied fields and currents, where the nucleation rate is well described by a modified Néel-Brown model in which

the energy barrier varies linearly with field and current.[41] In contrast, the depinning process is found to be influenced only by the applied fields and independent of the current over a wide range. This is consistent with an analytical model of a Néel wall and a micromagnetc simulation: Both predict that spin torques do not significantly change the energy barrier but instead only modify the micromagnetic structure of the pinned domain wall.

We would like to thank L. Buda-Prejbeanu for fruitful discussions and great help with the micromagnetic simulations. This work was supported by The Partner University Fund "Novel Magnetic Materials for Spin Torque Physics and Devices," the ANR-10-BLAN-1005 "Friends" and NSF Awards No. 1008654 and No. 1006575 as well as the European project MAGWIRE FP7-ICT-2009-5 257707 and the Region Lorraine.

[1] L. Berger, J. Appl. Phys. **49**, 2156 (1978); **50**, 2137 (1979).
[2] J. C. Slonczewski, J. Magn. Magn. Mater. **159**, L1 (1996); L. Berger, Phys. Rev. B **54**, 9353 (1996).
[3] J. A. Katine, F. J. Albert, R. A. Buhrman, E. B. Myers, and D. C. Ralph, Phys. Rev. Lett. **84**, 3149 (2000).
[4] M. Tsoi, A. G. M. Jansen, J. Bass, W.-C. Chiang, M. Seck, V. Tsoi, and P. Wyder, Phys. Rev. Lett. **80**, 4281 (1998).
[5] M. Tsoi, AGM Jansen, J. Bass, W. C. Chiang, V. Tsoi, and P. Wyder, Nature (London) **406**, 46 (2000).
[6] S. I. Kiselev, J. C. Sankey, I. N. Krivorotov, N. C. Emley, R. J. Schoelkopf, R. A. Buhrman, and D. C. Ralph, Nature (London) **425**, 380 (2003).
[7] D. C. Ralph and M. D. Stiles, J. Magn. Magn. Mater. **320**, 1190 (2008).
[8] C. H. Marrows, Adv. Phys. **54**, 585 (2005).
[9] G. S. D. Beach, M. Tsoi, and J. L. Erskine, J. Magn. Magn. Mater. **320**, 1272 (2008).
[10] D. A. Allwood, G. Xiong, C. C. Faulkner, D. Atkinson, D. Petit, and R. P. Cowburn, Science **309**, 1688 (2005).
[11] S. Parkin, M. Hayashi, and L. Thomas, Science **320**, 190 (2008).
[12] A. Yamaguchi, T. Ono, S. Nasu, K. Miyake, K. Mibu, and T. Shinjo, Phys. Rev. Lett. **92**, 077205 (2004).
[13] L. San Emeterio Alvarez, K.-Y. Wang, S. Lepadatu, S. Landi, S. J. Bending, and C. H. Marrows, Phys. Rev. Lett. **104**, 137205 (2010).
[14] C. Burrowes, A. P. Mihai, D. Ravelosona, J. V. Kim, C. Chappert, L. Vila, A. Marty, Y. Samson, F. Garcia-Sanchez, L. D. Buda-Prejbeanu, I. Tudosa, E. E. Fullerton, and J.-P. Attané, Nat. Phys. **6**, 17 (2010).
[15] V. K. Valev, M. Gruyters, A. Kirilyuk, and T. Rasing, Phys. Rev. Lett. **96**, 067206 (2009).
[16] R. M. Konik and Y. Adamov, Phys. Rev. Lett. **102**, 097203 (2009).
[17] A. Chanthbouala, R. Matsumoto, J. Grollier, V. Cros, A. Anane, A. Fert, A. V. Khvalovskiy, K. A. Zvezdin, K. Nishimura, Y. Nagamine, H. Maehara, K. Tsunekawa, A. Fukushima, and S. Yuasa, Nat. Phys. **10**, 1038 (2011).
[18] D. Ravelosona, S. Mangin, Y. Lemaho, J. A. Katine, B. D. Terris, and E. E. Fullerton, Phys. Rev. Lett **96**, 186604 (2006).
[19] D. Ravelosona, S. Mangin, J. A. Katine, E. E. Fullerton, and B. D. Terris, Appl. Phys. Lett. **90**, 072508 (2007).
[20] D. Ravelosona, S. Mangin, Y. Henry, Y. Lemaho, J. A. Katine, B. D. Terris, and E. E. Fullerton, J. Phys. D: Appl. Phys. **40**, 1253 (2007).
[21] D. P. Bernstein, B. Bräuer, R. Kukreja, J. Stöhr, T. Hauet, J. Cucchiara, S. Mangin, J. A. Katine, T. Tyliszczak, K. W. Chou, and Y. Acremann, Phys. Rev. B **83**, 180410(R) (2011).
[22] T. Koyama, D. Chiba, K. Ueda, K. Kondou, H. Tanigawa, S. Fukami, T. Suzuki, N. Ohshima, N. Ishiwata, Y. Nakatani, K. Kobayashi, and T. Ono, Nat. Mater. **10**, 194 (2011).
[23] R. Hiramatsu, K. Kondou, T. Koyama, Y. Yoshimura, D. Chiba, S. Fukami, N. Ishiwata, and T. Ono, Jpn. J. Appl. Phys. **51**, 028005 (2012).
[24] S. Mangin, D. Ravelosona, J. A. Katine, M. J. Carrey, B. D. Terris, and E. E. Fullerton, Nat. Mater. **5**, 210 (2006).
[25] J. Cucchiara, E. E. Fullerton, A. D. Kent, J. Z. Sun, Y. Henry, and S. Mangin, Phys. Rev. B **84**, 100405 (2011).
[26] S. Le Gall, J. Cucchiara, M. Gottwald, C. Berthelot, C. H. Lambert, Y. Henry, D. Bedau, D. B. Gopman, H. Liu, A. D. Kent, J. Z. Sun, W. Lin, D. Ravelosona, J. A. Katine, E. E. Fullerton, and S. Mangin, Phys. Rev. B **86**, 014419 (2012).
[27] P. Vischer *et al.*, J. Appl. Phys. **103**, 07A722 (2008).
[28] N. Reckers, J. Cucchiara, O. Posth, C. Hassel, F. M. Römer, R. Narkowicz, R. A. Gallardo, P. Landenos, H. Zahres, S. Mangin, J. A. Katine, E. E. Fullerton, G. Dum pich, R. Meckenstock, J. Lindner, and M. Farle, Phys. Rev B **83**, 184427 (2011).
[29] W. Lin, J. Cucchiara, C. Berthelot, T. Hauet, Y. Henry, J. A. Katine, Eric E. Fullerton, and S. Mangin, Appl. Phys. Lett. **96**, 252503 (2010).
[30] M. R. Scheinfein, LLG Micromagnetic Simulator, http://llgmicro.home.mindspring.com/, accessed 1 June 2011.
[31] S. Mangin, Y. Henry, D. Ravelosona, J. A. Katine, and E. E. Fullerton, Appl. Phys. Lett. **94**, 012502 (2009).
[32] D. B. Gopman, D. Bedau, S. Mangin, C. H. Lambert, E. E. Fullerton, J. A. Katine, and A. D. Kent, Appl. Phys. Lett. **100**, 062404 (2012).
[33] J. Cucchiara, Y. Henry, D. Ravelosona, D. Lacour, E. E. Fullerton, J. A. Katine, and S. Mangin, Appl. Phys. Lett. **94**, 102503 (2009).
[34] S. Mangin, G. Marchal, W. Wernsdorfer, A. Sulpice, K. Hasselbach, D. Mailly, and B. Barbara, Europhys. Lett. **39**, 675 (1997).
[35] S. Mangin, A. Sulpice, G. Marchal, C. Bellouard, W. Wernsdorfer, and B. Barbara, Phys. Rev. B **60**, 1204 (1999).
[36] D. Bedau, H. Liu, J.-J. Bouzaglou, A. D. Kent, J. Z. Sun, J. A. Katine, E. E. Fullerton, and S. Mangin, Appl. Phys. Lett. **96**, 022514 (2010).
[37] D. Bedau, H. Liu, J. Z. Sun, J. A. Katine, E. E. Fullerton, S. Mangin, and A. D. Kent, Appl. Phys. Lett. **97**, 262502 (2010).
[38] H. Liu, D. Bedau, J. Z. Sun, S. Mangin, E. E. Fullerton, J. A. Katine, and A. D. Kent, Phys. Rev. B **85**, 220405 (2012).
[39] J.-P. Jamet, S. Lemerle, P. Meyer, J. Ferré, B. Bartenlian, N. Bardou, C. Chappert, P. Veillet, F. Rousseaux, D. Decanini, and H. Launois, Phys. Rev. B **57**, 14320 (1998).
[40] J. Ferré, *Spin Dynamics in Confined Magnetic Structures I* (Springer, Berlin, 2002), Vol. 83, p. 127.
[41] Z. Li and S. Zhang, Phys. Rev. B **69**, 134416 (2004).
[42] J.-V. Kim and C. Burrowes, Phys. Rev. B **80**, 214424 (2009).
[43] A. Thiaville, Y. Nakatani, J. Miltat, and Y. Suzuki, Europhys. Lett. **69**, 990 (2005).